



## SIGNALS FOR PARITY VIOLATION IN THE ELECTROWEAK SYMMETRY BREAKING SECTOR

S. Dawson<sup>(a)\*</sup> and G. Valencia<sup>(b,c)</sup>

<sup>(a)</sup> *Physics Department, Brookhaven National Laboratory, Upton, NY 11973*

<sup>(b)</sup> *Theoretical Physics, Fermi National Accelerator Laboratory, Batavia, IL 60510*

<sup>(c)</sup> *Department of Physics, Iowa State University, Ames, IA 50011*

### Abstract

We consider the possibility of observing a parity violating but  $CP$  conserving interaction in the symmetry breaking sector of the electroweak theory. We find that the best probe for such an interaction is a forward-backward asymmetry in  $W^+W^-$  production from polarized  $e_R^-e_L^+$  collisions. An observable asymmetry would be strong evidence against a custodial  $SU(2)$  symmetry. We also discuss the effects of such an interaction in future  $e^- \gamma$  colliders as well as in rare decays of  $K$  and  $B$  mesons.

---

\*Work supported by the U.S. DOE under contract DE-AC02-76CH00016.



# 1 Introduction

The standard model of electroweak interactions has now been tested thoroughly in a number of experiments. The only missing ingredients are the top-quark and the Higgs-boson. Whereas we expect that the top-quark will be found in the near future, the same cannot be said for the Higgs-boson. The Higgs-boson in the standard model is responsible for the breaking of electroweak symmetry, and experiments conducted thus far have not tested directly the energy scales at which the symmetry breaking is thought to occur.

There are many different physics possibilities that could be responsible for the breaking of the electroweak symmetry. This makes it interesting to parameterize the symmetry breaking sector of the theory in a model independent way, and to explore the sensitivity of present and future experiments to the new physics. In general, one can divide the possibilities for the new physics into two classes. It is possible for the new interactions to remain weakly coupled. Such models typically contain new particles in the few-hundred GeV mass range. Examples are models with low energy supersymmetry [1]. It is also possible that there are no new particles below a few TeV and that the electroweak interactions become strong. We will focus on the second possibility, although some of our results apply in the first case as well.

We start from the minimal standard model without a Higgs boson. This model can be written as the usual standard model, but replacing the scalar sector with the effective Lagrangian [2]:

$$\mathcal{L}^{(2)} = \frac{v^2}{4} \text{Tr} \left( D^\mu \Sigma^\dagger D_\mu \Sigma \right). \quad (1)$$

The matrix  $\Sigma \equiv \exp(i\vec{w} \cdot \vec{\tau}/v)$ , contains the would-be Goldstone bosons  $w_i$  that give the  $W$  and  $Z$  their mass via the Higgs mechanism. They interact with the  $SU(2)_L \times U(1)_Y$  gauge bosons in a way dictated by the covariant derivative:

$$D_\mu \Sigma = \partial_\mu \Sigma + \frac{i}{2} g W_\mu^i \tau^i - \frac{i}{2} g' B_\mu \Sigma \tau_3. \quad (2)$$

Eq. 1 is thus an  $SU(2)_L \times U(1)_Y$  gauge invariant mass term for the  $W$  and  $Z$ . The physical masses are obtained with  $v \approx 246$  GeV. This non-linear realization of the symmetry breaking sector contains the same low energy physics as the minimal standard model when the Higgs-boson is taken to be very heavy [2]. It is a non-renormalizable interaction that is interpreted as an effective field theory, valid below some scale  $\Lambda$ . The details of the physics that break electroweak symmetry determine the next-to-leading order effective Lagrangian. At energies small compared to  $\Lambda$ , it is sufficient to consider those terms that are suppressed by  $E^2/\Lambda^2$  with respect to Eq. 1.

We have previously discussed the case in which the new physics contains a custodial  $SU(2)$  global symmetry that is broken only by the hypercharge coupling  $g'$  and by the mass splittings in the left handed  $SU(2)$  fermion doublets [3]. Furthermore, we specialized to the case of very high energy experiments in which the scalar interactions are stronger than the gauge interactions and it is consistent to set all the custodial

$SU(2)$  violating counterterms in the next-to-leading order effective Lagrangian to zero.

We now want to extend that analysis and study the effects of custodial  $SU(2)$  breaking counterterms. The one with the minimum number of derivatives, two, is:

$$\mathcal{L}^{(2)} = \frac{1}{8}\Delta\rho v^2 \left[ \text{Tr} \left( \tau_3 \Sigma^\dagger D_\mu \Sigma \right) \right]^2. \quad (3)$$

This term describes deviations of the  $\rho$  parameter from one<sup>2</sup> and has been studied at length in the literature. Unfortunately, there are many operators with four derivatives that break the custodial symmetry in the next-to-leading effective Lagrangian, making a general study quite complicated. A complete set of these operators has been given in Ref. [2, 5]. For specific problems, however, one finds that only a few operators are relevant. For example, for physics at LEP, only one of them contributes at tree-level to the so called “oblique” electroweak corrections expected to dominate in that context. It corresponds to the parameter “U” of Peskin and Takeuchi [6].

We will focus on a special operator, that apart from breaking the custodial symmetry, violates parity and charge conjugation while conserving CP. The interest of this operator lies in the fact that it is unique, and that violating parity, it can in principle produce signatures that will set it apart from the other next-to-leading terms in the effective Lagrangian. Furthermore, since the weak interactions violate parity, there is no reason to expect this operator to have the additional suppression factors usually associated with CP violation. Observation of substantial effects in the custodial  $SU(2)$  breaking sector of the theory would have significant implications in our understanding of electroweak symmetry breaking. In particular, models would have to explain the smallness of  $\Delta\rho$  in the absence of a custodial symmetry [7].

In Section 2, we present the parity violating Lagrangian which is the focus of our study and discuss the interactions which it generates. In Sections 3 and 4, we turn our attention to potential future colliders. Section 3 contains a particularly interesting result for asymmetries in polarized  $e^+e^-$  production of  $W$  boson pairs. In Section 4 we estimate the size of the effect for  $WZ$  production in an  $e^-\gamma$  collider. Rare  $K$  and  $B$  meson decays are discussed in Section 5. We show that the processes  $B_s \rightarrow \mu^+\mu^-$  and  $K^+ \rightarrow \pi^+\nu\bar{\nu}$  can be sensitive to the effects of the parity violating operator in the effective Lagrangian. Finally, Section 6 contains our conclusions.

## 2 $P$ and $C$ violating but $CP$ conserving Lagrangian

The effective Lagrangian with these properties is:

$$\mathcal{L} = \frac{\hat{\alpha} g v^2}{\Lambda^2} \epsilon^{\alpha\beta\mu\nu} \text{Tr} \left( \tau_3 \Sigma^\dagger D_\mu \Sigma \right) \text{Tr} \left( W_{\alpha\beta} D_\nu \Sigma \Sigma^\dagger \right), \quad (4)$$

---

<sup>2</sup>Experimentally,  $\Delta\rho = 0.0016 \pm 0.0032$  [4].

where  $W_{\mu\nu}$  is the  $SU(2)$  field strength tensor. In terms of  $W_\mu \equiv W_\mu^i \tau_i$ , it is given by:<sup>3</sup>

$$W_{\mu\nu} = \frac{1}{2} \left( \partial_\mu W_\nu - \partial_\nu W_\mu + \frac{i}{2} g [W_\mu, W_\nu] \right). \quad (5)$$

A similar operator, with  $B_{\alpha\beta}$  instead of  $W_{\alpha\beta}$  would read:

$$\begin{aligned} \mathcal{L} &= \frac{\hat{\alpha}' g' v^2}{\Lambda^2} \epsilon^{\alpha\beta\mu\nu} \text{Tr} \left( \tau_3 \Sigma^\dagger D_\mu \Sigma \right) \text{Tr} \left( B_{\alpha\beta} D_\nu \Sigma^\dagger \Sigma \right) \\ &= \frac{\hat{\alpha}' g' v^2}{2\Lambda^2} \epsilon^{\alpha\beta\mu\nu} B_{\alpha\beta} \text{Tr} \left( \tau_3 \Sigma^\dagger D_\mu \Sigma \right) \text{Tr} \left( \tau_3 D_\nu \Sigma^\dagger \Sigma \right), \end{aligned} \quad (6)$$

which is seen to vanish due to the antisymmetric nature of the epsilon tensor after using  $D_\nu \Sigma^\dagger \Sigma = -\Sigma^\dagger D_\nu \Sigma$ . Eq. 4 is the only term in the effective Lagrangian which violates parity and conserves  $CP$  to  $\mathcal{O}(E^4)$ .

The operator of Eq. 4 has been recently discussed by Appelquist and Wu [5], and the correspondence between our notation and theirs is  $\hat{\alpha} v^2 / \Lambda^2 = \alpha_{11}$ . The reason for the additional factor that we introduce, is that this operator arises at next-to-leading order (in the energy expansion), and is thus suppressed by the scale of new physics. In models where the operator is generated at one-loop, as the one discussed in Ref. [5], the suppression factor appears as  $16\pi^2$ . This corresponds to the usual “naive dimensional analysis” result  $\Lambda \approx 4\pi v$ .

It is instructive to consider the model of Ref. [5]. In this model, custodial  $SU(2)$  is broken by the splitting between the masses of new  $SU(2)$  fermion doublets  $m_U - m_D$ , and the size of  $\alpha_{11}$  is constrained by  $\Delta\rho$ . Requiring the new physics to contribute no more than a few percent to  $\Delta\rho$ , Ref. [5] finds  $\alpha_{11} \leq 2 \times 10^{-4}$ , which for  $\Lambda = 1$  TeV, corresponds to  $\hat{\alpha} \leq 3 \times 10^{-3}$ . In models where  $\Delta\rho$  is small as a consequence of an approximate custodial symmetry,  $\hat{\alpha}$  will have a natural size  $\hat{\alpha} \approx \Delta\rho$ . This is consistent with the power counting analysis we sketched in Ref. [3]. However, it is also possible, although not natural, to have  $\Delta\rho$  small without a custodial symmetry. In such models  $\hat{\alpha}$  would naturally be of order one.

In unitary gauge, the effects of the Lagrangian Eq. 4, are very simple. There is a three gauge boson interaction:

$$\mathcal{L}^{(3)} = -\frac{\hat{\alpha} g^3 v^2}{\Lambda^2 c_\theta} \epsilon^{\alpha\beta\mu\nu} \left( W_\nu^- \partial_\alpha W_\beta^+ - W_\beta^+ \partial_\alpha W_\nu^- \right) Z_\mu, \quad (7)$$

which generates the  $Z(q) \rightarrow W^+(p^+) W^-(p^-)$  “anomalous” coupling of Figure 1. In the notation of Ref.[8] we have the correspondence:

$$g_5^Z = \hat{\alpha} \frac{g^2 v^2}{c_\theta^2 \Lambda^2}. \quad (8)$$

There is also a four gauge boson interaction:

$$\mathcal{L}^{(4)} = i \frac{2\hat{\alpha} g^4 v^2 s_\theta}{\Lambda^2 c_\theta} \epsilon^{\alpha\beta\mu\nu} W_\alpha^- W_\beta^+ Z_\mu A_\nu. \quad (9)$$

---

<sup>3</sup>Notice that there is a typo in Eq. 2.1 of Ref. [3].

Some of the Feynman rules that can be derived from Eq. 4, are shown in Figure. 1. Our notation is  $s_\theta = \sin \theta_W$ ,  $c_\theta = \cos \theta_W$ .

Within the minimal standard model, the operator Eq. 4 is generated at one-loop by the splitting between top-quark and bottom-quark masses. In the limit  $m_t \gg m_W$ , and setting  $m_b = 0$ , we find from the diagram in Figure 2:

$$\left(\frac{v^2}{\Lambda^2} \hat{\alpha}\right)_{\text{top}} = \frac{|V_{tb}|^2}{128\pi^2} \left(1 - \frac{8}{3}s_\theta^2\right) \approx 3 \times 10^{-4} \quad (10)$$

Throughout our paper, we will express our results in terms of  $g_5^Z$  adhering to convention. However, we wish to emphasize that the reader should keep Eq. 8 in mind. This expression tells us the natural size of  $g_5^Z$ , and its relation to the new physics producing it. For example, if we assume that the new physics enters at 1 TeV, then  $g_5^Z \sim \mathcal{O}(10^{-2})$  in theories in which there is no custodial  $SU(2)$  and  $\Delta\rho$  is small accidentally. Similarly,  $g_5^Z \sim \mathcal{O}(10^{-4})$  in theories that have an approximate custodial  $SU(2)$ .

### 3 Forward-backward asymmetry in $e_L^+ e_R^- \rightarrow W^+ W^-$

In this section we study the effect of the parity violating operator Eq. 4 on the process  $e^+ e^- \rightarrow W^+ W^-$ . This process receives contributions from the diagrams of Figure 3. The  $t$  channel neutrino exchange diagram contributes only to  $e_L^- e_R^+ \rightarrow W^- W^+$ . We will treat separately the two electron polarizations, because as we will see, only the process with right-handed electrons generates a parity odd observable proportional to  $g_5^Z$ .

We start by writing down the amplitudes generated by the lowest order effective Lagrangian (Eq. 1 plus the kinetic energy terms for the gauge fields), and by the parity violating Lagrangian Eq. 4. For  $e_R^- e_L^+$  we find:

$$M(e_L^+ e_R^- \rightarrow W^+ W^-) = -\frac{g^2 s_\theta^2}{s(s - m_Z^2)} v_+^\alpha \epsilon^{*\mu}(p_3, \lambda^+) \epsilon^{*\nu}(p_4, \lambda^-) \cdot \left[ m_Z^2 \left( F_1^R g_{\mu\nu}(p_4 - p_3)_\alpha + F_3^R (q_\mu g_{\alpha\nu} - q_\nu g_{\alpha\mu}) \right) + i s F_5^R \epsilon_{\alpha\mu\nu\rho} (p_4 - p_3)^\rho \right] \quad (11)$$

where  $F_1^R = 1$ ,  $F_3^R = 2$ , and  $F_5^R = g_5^Z$ . For  $e_L^- e_R^+$  we find:

$$M(e_R^+ e_L^- \rightarrow W^+ W^-) = -v_-^\alpha \epsilon^{*\mu}(p_3, \lambda^+) \epsilon^{*\nu}(p_4, \lambda^-) \left\{ \frac{g^2 s_\theta^2}{s(s - m_Z^2)} \cdot \left[ m_Z^2 \left( F_1^L g_{\mu\nu}(p_4 - p_3)_\alpha + F_3^L (q_\mu g_{\alpha\nu} - q_\nu g_{\alpha\mu}) \right) + i s F_5^L \epsilon_{\alpha\mu\nu\rho} (p_4 - p_3)^\rho \right] + \frac{g^2}{2t} (p_1 - p_3)^\rho \left( g_{\mu\rho} g_{\nu\alpha} + g_{\nu\alpha} g_{\mu\rho} - g_{\alpha\rho} g_{\mu\nu} - i \epsilon_{\mu\rho\nu\alpha} \right) \right\} \quad (12)$$

where now:

$$F_1^L = F_3^L/2 = \left(1 - \frac{s}{m_Z^2} \frac{1}{2s_\theta^2}\right) \quad F_5^L = g_5^Z \left(1 - \frac{1}{2s_\theta^2}\right) \quad (13)$$

and  $s, t$  are the usual Mandelstam variables. We find it convenient to use the vector equivalence technique [9], in which the spinor expression  $\bar{v}_\pm(p_1)\gamma_\mu u_\pm(p_2)$  is replaced with the equivalent vector  $v_\pm = \sqrt{s}(0, 1, \mp i, 0)$  ( $v_+$  being a right-handed electron). This allows computation of the amplitudes by explicitly replacing expressions for all four-vectors in the  $e^+e^-$  center of mass frame.

We then find that the differential cross-section contains a parity-violating contribution from the interference of the  $g_5^Z$  term and the lowest order amplitude. It also contains a contribution proportional to  $|g_5^Z|^2$ . These contributions are present for both electron polarizations. However, the cross-section for left-handed electrons is much larger than the cross-section for right-handed electrons, and is not very sensitive to the value of  $g_5^Z$ . This is why the studies of unpolarized cross-sections in the literature have found the effect of  $g_5^Z$  to be less important than that of other (parity conserving) anomalous couplings.

We will show that the cross-section with right-handed electrons is much more sensitive to  $g_5^Z$  than the unpolarized cross-section is. However, deviations of the cross-section (polarized or not) from its minimal standard model value can also be due to any of the parity conserving anomalous couplings that we have ignored.

Of greater interest to us will be the fact that the parity violating operator introduces a forward-backward asymmetry that is not present in the minimal standard model for the case of right-handed electrons (except, of course, for its one-loop contribution to  $g_5^Z$  Eq. 10). This forward-backward asymmetry is a parity odd observable that is not affected by the other anomalous couplings that we have ignored and it is, therefore, the best place to search for  $g_5^Z$ .

The differential cross-section for right-handed electrons is given by:

$$\begin{aligned} \left. \frac{d\sigma_{TT}}{d(\cos\theta)} \right|_{e_R^-} &= \frac{\pi\alpha^2}{s} \beta^3 \frac{m_Z^4}{(s - m_Z^2)^2} \sin^2\theta \\ \left. \frac{d\sigma_{LL}}{d(\cos\theta)} \right|_{e_R^-} &= \frac{\pi\alpha^2}{32s} \frac{\beta^3}{c_\theta^4} \frac{s^2}{(s - m_Z^2)^2} (5 + \beta^2)^2 \sin^2\theta \\ \left. \frac{d\sigma_{TL}}{d(\cos\theta)} \right|_{e_R^-} &= \frac{\pi\alpha^2}{s} \frac{\beta^3}{c_\theta^2} \frac{m_Z^2 s}{(s - m_Z^2)^2} \left( 1 + \cos^2\theta + 2\beta \frac{s}{m_Z^2} g_5^Z \cos\theta \right) \end{aligned} \quad (14)$$

where we use the notation  $\beta^2 = 1 - 4m_W^2/s$ . We have summed over the different polarization states that contribute to the cross sections with two transversely polarized  $W$ 's in the final state,  $\sigma_{TT}$ , and with one transversely and one longitudinally polarized  $W$ 's in the final state,  $\sigma_{TL}$ . Our result agrees with that of Ahn *et. al.*[10].<sup>4</sup> In terms of the notation of Ref. [10], our result contains only the tree-level standard model values of  $F_1$  and  $F_3$ , and we have only written terms that are linear in  $g_5^Z$  (but our numerical results also include the terms quadratic in  $g_5^Z$ ). Other anomalous couplings do not contribute to the forward backward asymmetry in  $e_R^- e_L^+ \rightarrow W^- W^+$  and they are not considered here.

<sup>4</sup>Except for what appears to be a typo in Eq. 2.10 of Ref. [10] where we find that  $A_3$  goes like  $\beta$  and not like  $\beta^2$ .

As can be seen from Eq. 14, there is a term in  $\sigma_{TL}$  that is linear in  $\cos\theta$  (the scattering angle in the center of mass). This term arises from the interference of  $F_3$  and  $F_5$  and gives rise to a forward-backward asymmetry. Although there is a similar term in the differential cross-section for  $e_L^- e_R^+ \rightarrow W^+ W^-$ , in that case one also has a  $t$ -channel neutrino exchange diagram that gives rise to a very large forward-backward asymmetry within the minimal standard model. Thus, if we want to isolate the  $g_5^Z$  term, it is very important to have right-handed electrons. Since the cross-section for left-handed electrons is several orders of magnitude larger than that for right-handed electrons, it presents a formidable background. In Figure 4, we show the results for the cross-section at  $\sqrt{s} = 200$  GeV,  $\sqrt{s} = 500$  GeV and  $\sqrt{s} = 1$  TeV respectively. In these figures we assume that the electron beam has a fraction  $P_R$  of right-handed electrons and  $(1 - P_R)$  of left-handed electrons. We can see that only the cross-section for right-handed electrons is sensitive to the value of  $g_5^Z$ , and that this sensitivity increases with increasing center of mass energy.

In Figure 5 we show the forward-backward asymmetry for  $\sqrt{s} = 200$  GeV, 500 GeV, and 1 TeV. Again we find that the greatest sensitivity to  $g_5^Z$  occurs for right-handed electrons, and that this sensitivity increases with increasing center of mass energy. However, in this case we see that as long as one has a high degree of polarization, even the lower energy machines could place a good bound on  $g_5^Z$ .

A detailed phenomenological study of this process would have to address the issue of reconstruction of the scattering angle  $\theta$  after the  $W$ 's decay. It may also be possible to enhance the sensitivity to  $g_5^Z$  by using the fact that the forward-backward asymmetry is present only in  $\sigma_{TL}$ .

#### 4 $e^- \gamma \rightarrow \nu W^- Z$

In this section we explore the possibility of observing the effects of the parity violating operator Eq. 4 via the anomalous four-gauge-boson coupling that it generates. We thus turn our attention to high energy vector-boson fusion experiments. Given the form of the four vector-boson interaction, Eq. 9, we look at processes involving one photon and one  $Z$ . There are several possibilities, for example  $Z\gamma$  production in high energy  $e^+e^-$  or  $pp$  colliders. This process, however, suffers from large standard model backgrounds. We will study instead an idealized situation where we can isolate the effects of the new interaction as much as possible from the backgrounds. We consider a high energy  $e^- \gamma$  collider where we can cleanly identify the process  $e^- \gamma \rightarrow \nu W^- Z$ , and where we can also consider a polarized photon if need be. Some of the diagrams that give rise to this process are shown in Figure 6.

The new interaction contributes both to the vector-boson fusion diagrams, Figure 6a, and to the diagram that involves a three-gauge boson vertex, Figure 6b. This interplay of three and four-gauge-boson couplings from the same new operator makes the importance of a gauge invariant formulation of the effective Lagrangian manifest.

As a first approximation, we will use the equivalence theorem to replace the final state  $W$  and  $Z$  bosons by their corresponding Goldstone bosons,  $w$  and  $z$ . We first

compute the process  $W\gamma \rightarrow wz$ . The effective  $W$  approximation is then used to fold the sub-process cross section with the distribution of  $W$ 's in the electron [11].

The leading order amplitude (generated from Eq. 1) has been computed by us in Ref. [3]. To that contribution we add the amplitude generated by Eq. 4 to find (for  $s \gg m_W^2$ ):

$$M(W^-(q_1)\gamma(q_2) \rightarrow w^-(p_3)z(p_4)) = \epsilon^\mu(q_1, \lambda^W)\epsilon^\nu(q_2, \lambda^\gamma)g^2s_\theta \left[ \frac{2}{us} \left( \frac{ut}{2}g_{\mu\nu} + up_{3\mu}q_{1\nu} + tq_{2\mu}p_{3\nu} + sp_{3\mu}p_{3\nu} \right) - i\frac{2|g_5^Z|^2c_\theta^2}{m_W^2}\epsilon_{\mu\nu\alpha\beta}q_2^\alpha p_4^\beta \right] \quad (15)$$

The polarized cross sections,  $\sigma(\lambda^W, \lambda^\gamma)$ , are then:

$$\begin{aligned} \sigma_{+-} &= \sigma_{-+} = \frac{\pi\alpha^2}{s_\theta^2} \frac{1}{3s} \\ \sigma_{++} &= \sigma_{--} = \frac{\pi\alpha^2}{s_\theta^2} \frac{1}{3s} \left( |g_5^Z|^2 c_\theta^4 \frac{s^2}{m_W^4} \right) \\ \sigma_{L+} &= \sigma_{L-} = \frac{\pi\alpha^2}{s_\theta^2} \frac{1}{3s} \left( |g_5^Z|^2 \frac{c_\theta^4}{4} \frac{s^3}{m_W^6} \right) \end{aligned} \quad (16)$$

We fold these cross-sections with the luminosity for longitudinal and transverse  $W$ 's in an electron to obtain the effective- $W$  approximation result shown in Figure 7. This figure indicates a potential sensitivity of this process to values of  $g_5^Z < 0.1$  which are within the interesting range.

The subprocess cross-sections are identical for the different photon polarizations if we sum over the  $W$  polarization. However, in the exact process  $e^-\gamma \rightarrow \nu w^- z$  the cross-section depends on the photon polarization. Within the effective- $W$  approximation this dependence is also present because the polarized cross-sections of Eq. 16 are weighted by different factors: the distribution of  $W$ 's in the electron depends on the  $W$  polarization. This is also seen in Figure 7.

From Eq. 16 we can see that the new term does not interfere with the lowest order term: there is no contribution linear in  $g_5^Z$ . This means that we can only construct observables sensitive to  $g_5^Z$  that are parity even and can thus be generated by other anomalous couplings. Recall from Ref. [3], that the amplitude Eq. 15 receives contributions from the next-to-leading order operators  $L_{9L}$ ,  $L_{9R}$ , and  $L_{10}$ ; and that these contributions do interfere with the leading amplitude. Nevertheless, it is possible that the cross-section is more sensitive to the  $|g_5^Z|^2$  term than to those terms proportional to  $L_{9L}$ ,  $L_{9R}$  or  $L_{10}$  in very high energy machines. The reason for this is that the  $|g_5^Z|^2$  term is the only one that contributes to the amplitude where all three vector-bosons are longitudinally polarized (this is the source of  $\sigma_{L\pm}$  in Eq. 16) and we expect these terms of ‘‘enhanced electroweak strength’’ to dominate at high energies.

To construct an observable that can single out the  $g_5^Z$  coupling we need a term in the differential cross-section linear in  $g_5^Z$ . If we go beyond the effective- $W$  approximation, the new term proportional to  $g_5^Z$  will interfere with the lowest order amplitude through the parity violating term in the fermionic structure function [12]. Going beyond the effective- $W$  approximation requires the inclusion of the diagram in Figure 6b

as well. The interference term, not being present in the effective- $W$  approximation, is thus kinematically suppressed.

It appears that this process can potentially place significant constraints on  $g_5^Z$ , but a detailed phenomenological study of the real process  $e^- \gamma \rightarrow \nu W^- Z$  and its backgrounds is needed to draw any conclusions.

## 5 Rare $K$ - and $B$ -meson decays

These rare decays receive contributions from the parity violating effective Lagrangian Eq. 4 at the one-loop level. One-loop amplitudes with one vertex from the  $\mathcal{O}(E^4)$  effective Lagrangian are  $\mathcal{O}(E^6)$ . A complete study thus requires the next to next to leading order counterterms, as well as two loop contributions from the leading order effective Lagrangian. However, we will find that our one-loop amplitudes are finite so we will be able to draw some conclusions from our incomplete analysis. As a minimal consistency check, we first look at the effects on the gauge boson self-energies that could arise at the same order. This involves, for example, the potential contributions to  $\Delta\rho$  from one-loop diagrams with one next-to-leading ( $g_5^Z$ ) vertex. However, one can easily see that there are no contributions to the gauge boson self-energies linear in  $g_5^Z$ . This is evident, as there are not enough independent four-vectors to saturate the indices of the epsilon tensor. A contribution to the self-energies (and to  $\Delta\rho$ ) quadratic in  $g_5^Z$  needs two next-to-leading vertices, and is therefore one-order higher in perturbation theory ( $\mathcal{O}(E^8)$  in our notation).

As is well known, the effective operators responsible for rare meson decays arise from box and penguin diagrams [13]. Since the lowest order effective Lagrangian (complete with fermions), and the new term Eq. 4, are separately gauge invariant, we are free to treat the two terms independently. We argued that the lowest order effective Lagrangian is just what remains when one removes the Higgs-boson from the standard model by taking its mass to infinity. However, it is easy to convince oneself that the standard model operators responsible for rare  $K$  and  $B$  decays do not depend on the Higgs-boson interactions. This is a consequence of the usual approximation in which external quark masses and momenta are set to zero. This means that, for example, Higgs-penguin diagrams in which a Higgs-boson couples to  $W$ 's or to top-quarks vanish in the limit of vanishing external quark masses and momenta. Since we will work in this approximation, our lowest order effective Lagrangian will simply reproduce the minimal standard model results which are usually obtained in  $R_\xi$  gauges.

As we said, the new term Eq. 4 is separately gauge invariant, so we may choose to perform the calculations involving this term in any other gauge. The simplest thing for us will be to perform them in unitary gauge. In this gauge Eq. 4 enters only through the anomalous  $ZW^+W^-$  coupling in the “Z-penguin” diagram of Figure 8 at the one-loop level.

For a heavy top-quark, we can ignore the contributions of charm and up-quarks in the intermediate state. The one-loop amplitude that contributes to the rare decays

is finite due to the GIM cancelation as noted by He [14]. We obtain for the effective one-loop vertex of Figure 8:

$$i\Gamma_{\text{PV}}^\mu = -i\frac{4G_F}{\sqrt{2}}\frac{\alpha}{2\pi s_\theta^2}M_Z^2c_\theta V_{ti}V_{tj}^*\left(g\hat{\alpha}\frac{v^2}{\Lambda^2}\right)W(x_t)\bar{v}_i\gamma^\mu(1-\gamma_5)u_j \quad (17)$$

where  $x_t = m_t^2/m_W^2$  and we have defined

$$W(x_t) \equiv \frac{3}{4}x_t\left(\frac{1}{1-x_t} + \frac{x_t \log x_t}{(1-x_t)^2}\right) \quad (18)$$

Our result agrees with that of Ref. [14]. This contribution to the rare decays modifies the standard model results for  $K_L, B^0 \rightarrow \ell^+\ell^-$ . In the notation of Ref.[16], the full results (leading order plus new contribution) are obtained by replacing:

$$\begin{aligned} Y(x_t) &\rightarrow \hat{Y}(x_t) = Y(x_t) + g_5^Z c_\theta^2 W(x_t) \\ Y(x_t) &= \frac{x_t}{8}\left(\frac{x_t-4}{x_t-1} + \frac{3x_t}{(x_t-1)^2}\log x_t\right) \end{aligned} \quad (19)$$

The case of  $K_L \rightarrow \mu^+\mu^-$  was discussed by He [14]. This mode, however, has a large long distance contribution due to a two-photon intermediate state that dominates the rate, and that is unaffected by the new couplings. Although one can compute reliably the absorptive part of the long distance component, at present one cannot compute its dispersive part. It is therefore not possible to place significant constraints on the short distance component (and thus on  $g_5^Z$ ) from the *measured* rate for this mode. Thus, the constraint obtained by He is purely theoretical, and it is equivalent to requiring that the new contribution be at most as large as the standard model short distance part. For  $m_t = 150$  GeV,  $Y(x_t) \approx W(x_t)$  so this implies:

$$g_5^Z \sim \mathcal{O}(1) \quad (20)$$

which is not a very stringent result if, as one expects,  $\Lambda \geq 1$  TeV.

A much better process to bound this contribution is  $B_s \rightarrow \mu^+\mu^-$  because the rate is dominated by short distance physics, and is therefore free of large theoretical uncertainties. This will allow us to obtain an experimental bound on the anomalous coupling once this process is measured. It will be a bound that can be improved by improving the accuracy of the measurement. The rate for this process is given by <sup>5</sup>:

$$\Gamma(B_s \rightarrow \mu^+\mu^-) = \frac{G_F^2}{\pi}\left(\frac{\alpha}{4\pi s_\theta^2}\right)^2 F_B^2 m_\mu^2 m_B |V_{tb}V_{ts}^*|^2 \hat{Y}(x_t)^2 \quad (21)$$

Numerically we use the Wolfenstein parameterization of the CKM matrix with  $A = .9$  and  $\lambda = .22$ . Our normalization for  $F_B$  is that in which  $f_\pi = 132$  MeV, we use  $F_B = 200$  MeV. Although this process has a very small rate, it has a very clean signature and should be seen in experiments at hadronic colliders with vertex detection. It

<sup>5</sup>Our standard model result agrees with that of Ref. [15, 16].

is conceivable that a precision measurement of this rate will exist in the future. In Figure 9 we have plotted the rate as a function of  $g_5^Z$ . This figure confirms what one expects from Eq. 19: a measurement of the rate to within factors of two can only bound  $g_5^Z$  to  $\mathcal{O}(1)$ . We can see from the figure that the sensitivity to  $g_5^Z$  increases with increasing top-quark mass. It is also evident that a significant constraint on  $g_5^Z$  can only be placed by a precision measurement once the top-quark mass and the CKM angles are known accurately.

The new vertex also contributes to the process  $K^+ \rightarrow \pi^+ \nu \bar{\nu}$ . This process is also dominated by short distance physics so its precise measurement would allow us to place significant constraints on  $g_5^Z$  (or  $\hat{\alpha}$ ). If we use the notation of Buras *et. al.*[17] for the standard model result, we find the full rate with the replacement:

$$\begin{aligned} X(x_t) &\rightarrow \hat{X}(x_t) = X(x_t) + g_5^Z c_\theta^2 W(x_t) \\ X(x_t) &= \frac{x_t}{8} \left( \frac{x_t + 2}{x_t - 1} + \frac{3x_t - 6}{(x_t - 1)^2} \log x_t \right) \end{aligned} \quad (22)$$

in the contribution from a top-quark intermediate state, which becomes:

$$\frac{B(K^+ \rightarrow \pi^+ \nu \bar{\nu})}{B(K^+ \rightarrow \pi^0 e^+ \nu)} = \left( \frac{\alpha}{\pi s_\theta^2} \right)^2 \frac{|V_{td} V_{ts}^*|^2}{|V_{us}|^2} \hat{X}(x_t)^2 \quad (23)$$

for each neutrino flavor. In Figure 10 we have included the standard model charm-quark contribution with QCD corrections as given in Ref. [17] for typical values of all unknown parameters. We see that this process will easily place bounds of  $\mathcal{O}(1)$  on  $g_5^Z$ , but that only a precision measurement combined with detailed knowledge of the top-quark mass, CKM angles, and QCD corrections could place significant constraints on  $g_5^Z$ .

As pointed out by He [14], there is another anomalous three-gauge-boson coupling,  $g_1^Z - 1$  in the notation of Ref. [8], that contributes to these processes at leading order in  $m_{\text{ext}}^2/m_W^2$ . A deviation from the standard model rate in these processes would, therefore, not be a definite signal for  $g_5^Z$ .

## 6 Conclusions

We have studied the possibility of observing the leading parity violating operator in an effective Lagrangian description of the symmetry breaking sector of the electroweak interactions. We have considered several observables that are even under parity and that would not distinguish between the effect of the parity violating interaction and a parity conserving one. We have also studied one observable (the forward backward asymmetry in  $e_L^+ e_R^- \rightarrow W^+ W^-$ ) that is odd under parity and would thus signal exclusively the parity violating interaction.

The parity violating operator also breaks custodial  $SU(2)$  symmetry, and therefore its natural size depends on whether the fundamental theory has a custodial symmetry or not. In theories with a custodial symmetry (or an approximate one), we expect

$g_5^Z$  to be  $\mathcal{O}(10^{-4})$  whereas without a custodial symmetry it could be  $\mathcal{O}(10^{-2})$ . The minimal standard model generates  $g_5^Z$  at one-loop at the  $10^{-4}$  level.

The most promising place to look for a non-zero value of  $g_5^Z$  is a forward-backward asymmetry in polarized  $e_R^- e_L^+$  collisions. The sensitivity of this asymmetry to  $g_5^Z$  is significantly reduced when the polarization of the electron beam is not near 100%. The asymmetry is sensitive to  $g_5^Z$  in machines with a center of mass energy as low as 200 GeV, but a much better sensitivity is obtained at higher energies. At higher energies, the total cross-section is also sensitive to  $g_5^Z$  provided that there is a high degree of  $e_R^-$  polarization.

We found that in addition to the usual anomalous three gauge boson vertex associated with  $g_5^Z$ , gauge invariance requires the existence of a four gauge boson vertex  $\gamma Z W^+ W^-$  that is also proportional to  $g_5^Z$ . We performed a preliminary study of the sensitivity of an  $e\gamma$  collider to  $g_5^Z$  that makes use of this new coupling. We find that at very high energies there is an increased sensitivity to  $g_5^Z$  because the new operator contains a coupling of the photon to three longitudinal vector bosons not present in the minimal standard model. The enhanced interactions of longitudinal vector bosons at high energies are thus the origin of the potentially large sensitivity of the process  $e^- \gamma \rightarrow \nu W^- Z$  to  $g_5^Z$ .

We find that the rare decays  $B_s \rightarrow \mu^+ \mu^-$  and  $K^+ \rightarrow \pi^+ \nu \bar{\nu}$  can easily place bounds of  $\mathcal{O}(1)$  on  $g_5^Z$ , but that to improve this, one needs a precise measurement of the rate combined with knowledge of all the standard model parameters.

A search for  $g_5^Z$  in these observables would yield valuable information on the electroweak symmetry breaking sector. In particular, an observation of a non-zero  $g_5^Z$  would be strong evidence against a custodial  $SU(2)$  symmetry.

### Acknowledgments

We are grateful to Tao Han, Xiao-Gang He and Eran Yehudai for useful discussions.

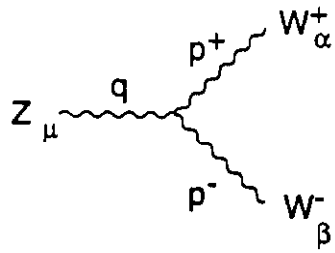
## References

- [1] For a list of references see J. Gunion et al, *The Higgs' Hunter's Guide*, (Addison-Wesley, Menlo Park, 1990.)
- [2] T. Appelquist and C. Bernard, *Phys. Rev.* **D22** 200 (1980); A. Longhitano, *Nucl. Phys.* **B188** 118 (1981).
- [3] J. Bagger, S. Dawson and G. Valencia, *Nucl. Phys.* **B399** 364 (1993).
- [4] See for example G. Altarelli, R. Barbieri and S. Jadach, *Nucl. Phys.* **B369** 3 (1992).
- [5] T. Appelquist and G.-H. Wu, YCTP-P7-93.
- [6] M. Peskin and T. Takeuchi, *Phys. Rev. Lett.* **65** 964 (1990); B. Holdom, *Phys. Lett.* **259B** 329 (1991).

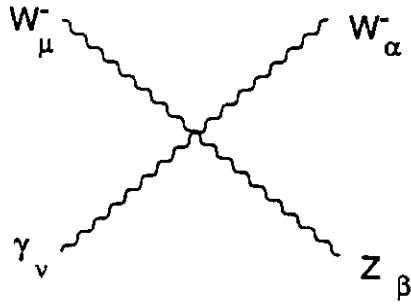
- [7] P. Sikivie, *et. al.*, *Nucl. Phys.* **B173** 189 (1980).
- [8] K. Hagiwara, *et. al.*, *Nucl. Phys.* **B282** 253 (1987). Recent discussions of theoretical issues regarding the parametrization of Hagiwara *et. al.* include: M. Einhorn and J. Wudka, Talk given at the workshop on electroweak symmetry breaking, Hiroshima, Japan (1991); C. Burgess and D. London, *Phys. Rev. Lett.* **69** 3428 (1992). A recent study of anomalous couplings in  $e^+e^-$  colliders using the effective Lagrangian formalism we use is B. Holdom, *Phys. Lett.* **258B** 156 (1991).
- [9] E. Yehudai, Fermilab-Pub-92/256-T (1992); SLAC-Report 383, PhD Thesis (1991).
- [10] C. Ahn, *et. al.*, *Nucl. Phys.* **B309** 221 (1988).
- [11] S. Dawson, *Nucl. Phys.* **B249** 42 (1985); M. Chanowitz and M. Gaillard, *Phys. Lett.* **142B** 85 (1984); G. Kane, W. Repko and W. Rolnick, *Phys. Lett.* **148B** 367 (1984).
- [12] T. Han, G. Valencia and S. Willenbrock, *Phys. Rev. Lett.* **69** 3274 (1992).
- [13] T. Inami and C. S. Lim, *Prog. Theor. Phys.* **65** 297 (1981); *ibid* **65** 1772 (1981).
- [14] Xiao-Gang He, UM-P-93/58, OZ-93/13 (1993).
- [15] M. Savage, *Phys. Lett.* **266B** 135 (1991).
- [16] G. Buchalla and A. Buras, *Nucl. Phys.* **B400** 225 (1993).
- [17] G. Buchalla, A. Buras and M. Harlander, *Nucl. Phys.* **B349** 1 (1991).

## FIGURE CAPTIONS

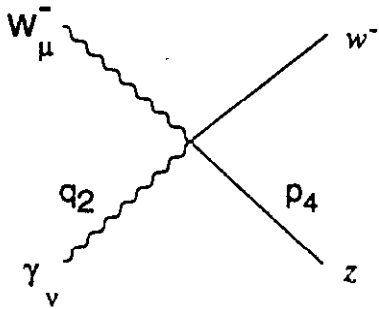
1. Feynman rules from Eq. 4. We show the two vertices that appear in unitary gauge, as well as some vertices involving would-be Goldstone bosons that we use. The notation in the figure is  $s_\theta^2 = \sin^2 \theta_W = .23$ ,  $c_\theta = \cos \theta_W$ . Our convention is that all momenta labelled  $q$  enter into the vertex, and all labelled  $p$  leave the vertex.
2. One-loop contribution to  $g_5^Z$  in the minimal standard model.
3. Diagrams contributing to  $e^+e^- \rightarrow W^+W^-$ . The full circle in the first diagram represents the three gauge boson vertex both from leading order and Eq. 4.
4. Total cross-section for the process  $e^+e^- \rightarrow W^+W^-$  for a)  $\sqrt{s} = 200$  GeV, b)  $\sqrt{s} = 500$  GeV and c)  $\sqrt{s} = 1$  TeV. The different curves from upper most to lowest correspond to a fraction of right handed electrons in the beam of 0%, 90%, 95%, 99% and 100%.
5. Forward-backward asymmetry for the process  $e^+e^- \rightarrow W^+W^-$  for a)  $\sqrt{s} = 200$  GeV, b)  $\sqrt{s} = 500$  GeV and c)  $\sqrt{s} = 1$  TeV. The different curves from upper most to lowest correspond to a fraction of right handed electrons in the beam of 0%, 90%, 95%, 99% and 100%.
6. Types of diagrams contributing to  $e^-\gamma \rightarrow \nu W^- Z$ . a) Diagrams with the vector-boson fusion topology (including both contact terms and  $s$ -and- $t$ -channel gauge boson exchanges. b) Diagram with a three gauge boson vertex that contributes to the process  $e^-\gamma \rightarrow \nu w^- z$  beyond the effective- $W$  approximation.
7.  $e^-\gamma \rightarrow \nu w^- z$  cross-section in the effective- $W$  approximation. We plot separately the results for each photon polarization with  $g_5^Z = 0$  (lower curves) and with  $g_5^Z = 0.1$ . For  $g_5^Z = 0.1$  the upper curve corresponds to  $\lambda_+^\gamma$  and the lower curve to  $\lambda_-^\gamma$ . For  $g_5^Z = 0$  the upper curve corresponds to  $\lambda_-^\gamma$  and the lower curve to  $\lambda_+^\gamma$ .
8. One-loop contribution from Eq. 4 to the  $\bar{d}_i d_j Z$  effective vertex. The effective three gauge boson vertex is represented by the full circle.
9. Rate for  $B_s \rightarrow \mu^+ \mu^-$  as a function of  $g_5^Z$ . The dashed curve corresponds to  $m_t = 200$  GeV, the dotted curve to  $m_t = 150$  GeV and the solid curve to  $m_t = 100$  GeV.
10.  $B(K^+ \rightarrow \pi^+ \nu \bar{\nu})$  as a function of  $g_5^Z$ . As an example we use  $\rho = 0$ ,  $\eta = .4$ ,  $V_{cb} = .041$ ,  $\Lambda_{QCD} = 200$  MeV, and  $m_c = 1.4$  GeV following Ref. [17]. The dashed curve corresponds to  $m_t = 200$  GeV, the dotted curve to  $m_t = 150$  GeV and the solid curve to  $m_t = 100$  GeV.



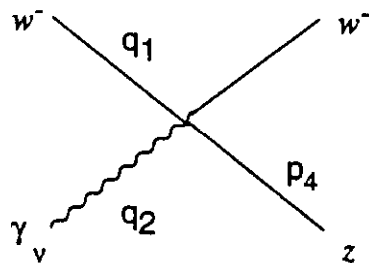
$$= g c_\theta g_5^z \epsilon^{\alpha\mu\beta\rho} (p^+ - p^-)_\rho$$



$$= -2g^2 s_\theta c_\theta g_5^z \epsilon^{\mu\nu\alpha\beta}$$



$$= 2g^2 s_\theta c_\theta^2 g_5^z / M_W^2 \epsilon^{\alpha\beta\mu\nu} q_{2\alpha} p_{4\beta}$$



$$= i 2g^2 s_\theta c_\theta^2 g_5^z / M_W^3 \epsilon^{\alpha\beta\mu\nu} q_{1\mu} q_{2\alpha} p_{4\beta}$$

Figure 1

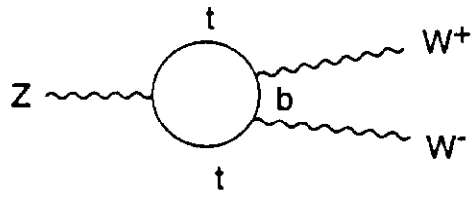


Figure 2

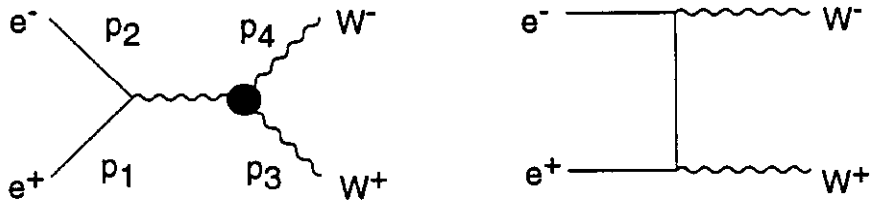


Figure 3

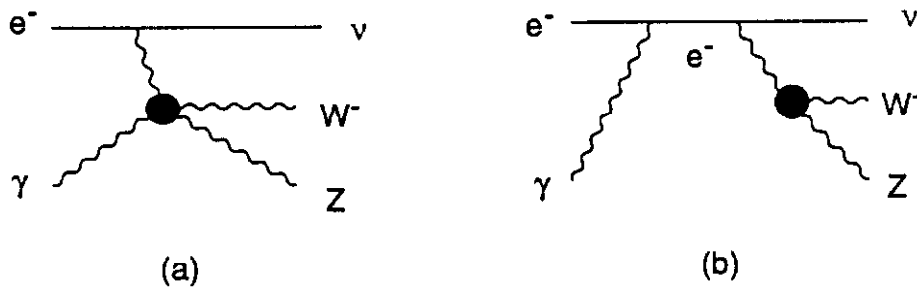


Figure 6

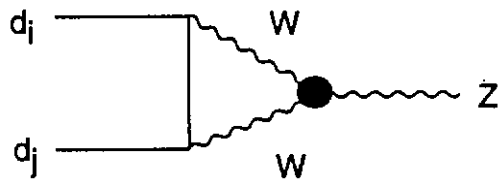


Figure 8

Figure 4a

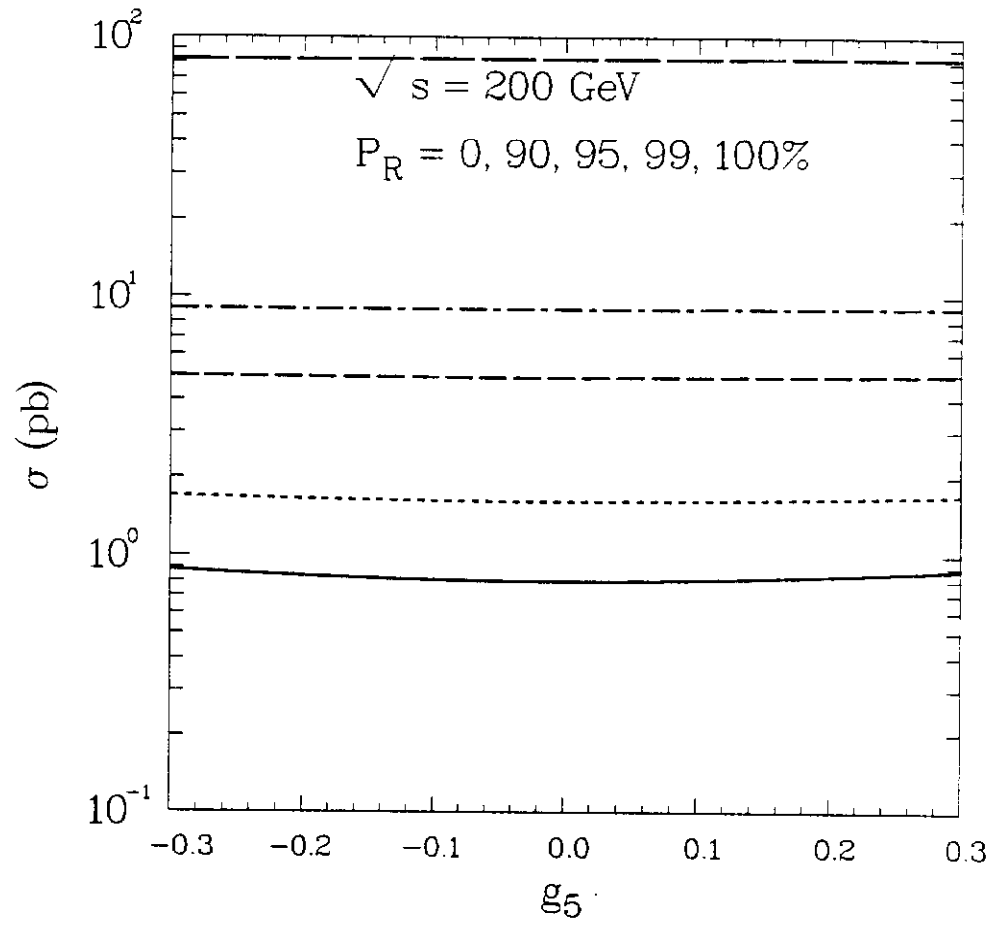


Figure 4b

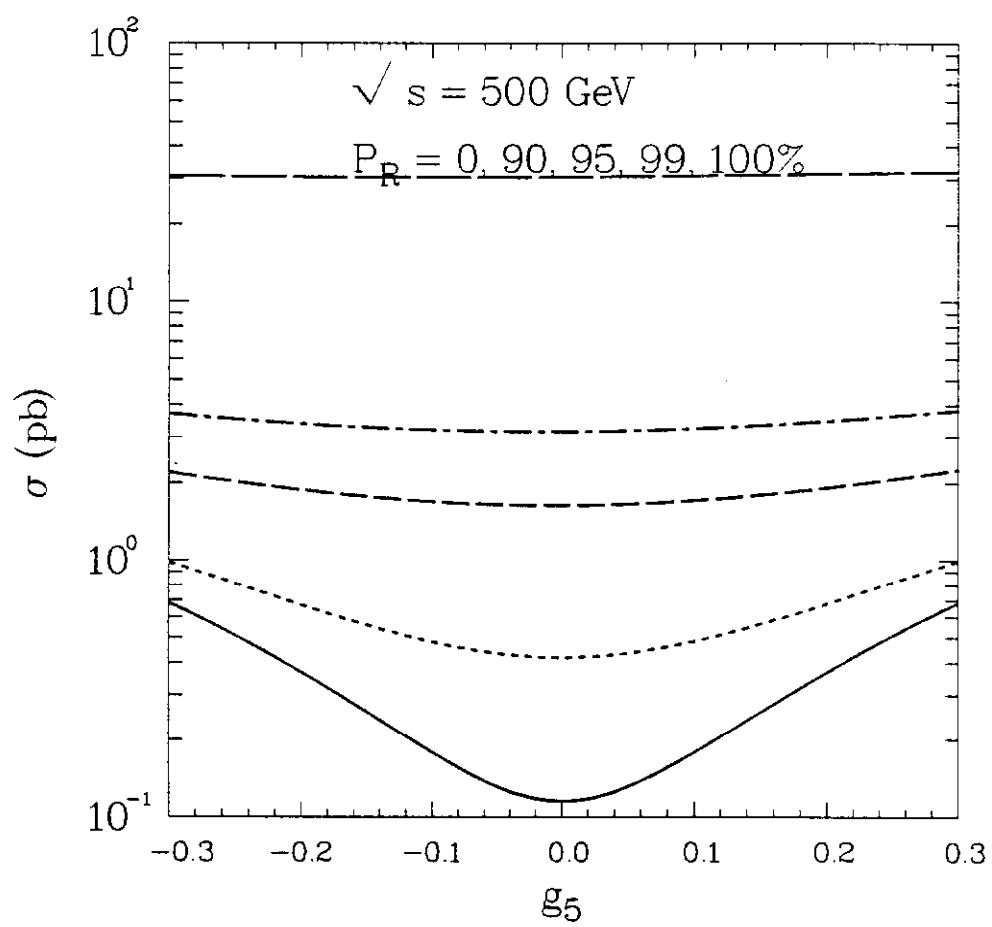


Figure 4c

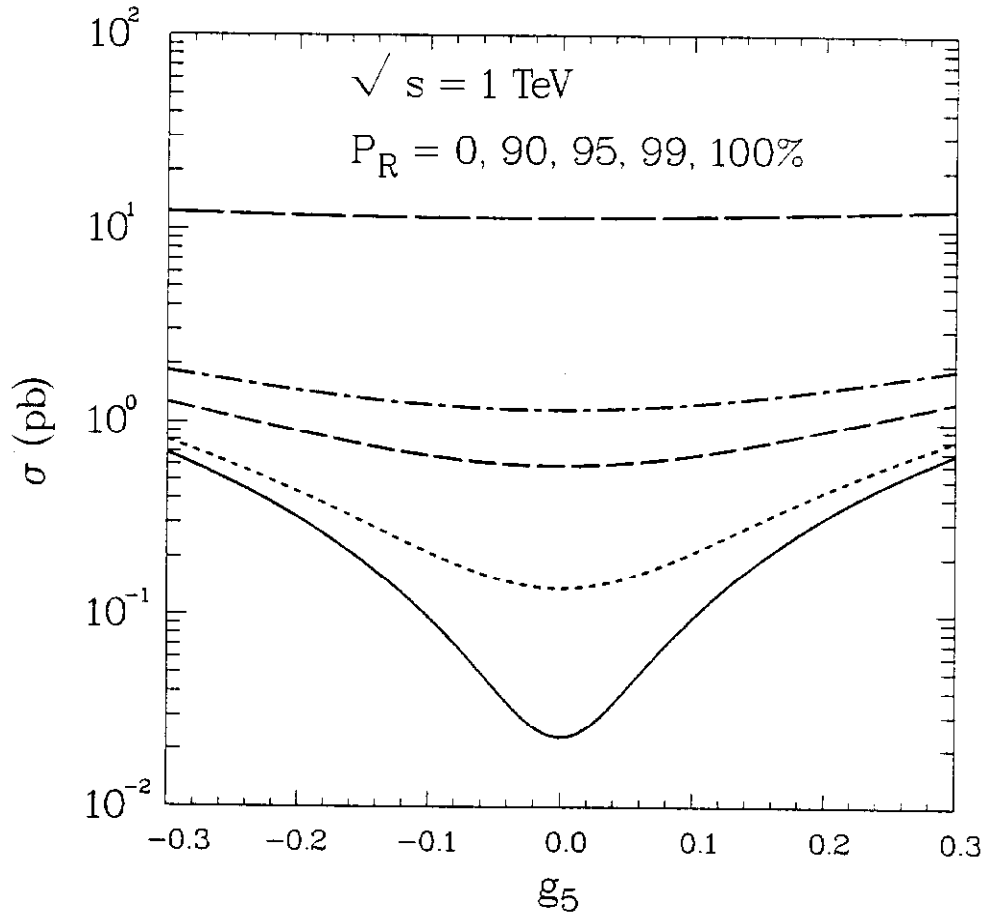


Figure 5a

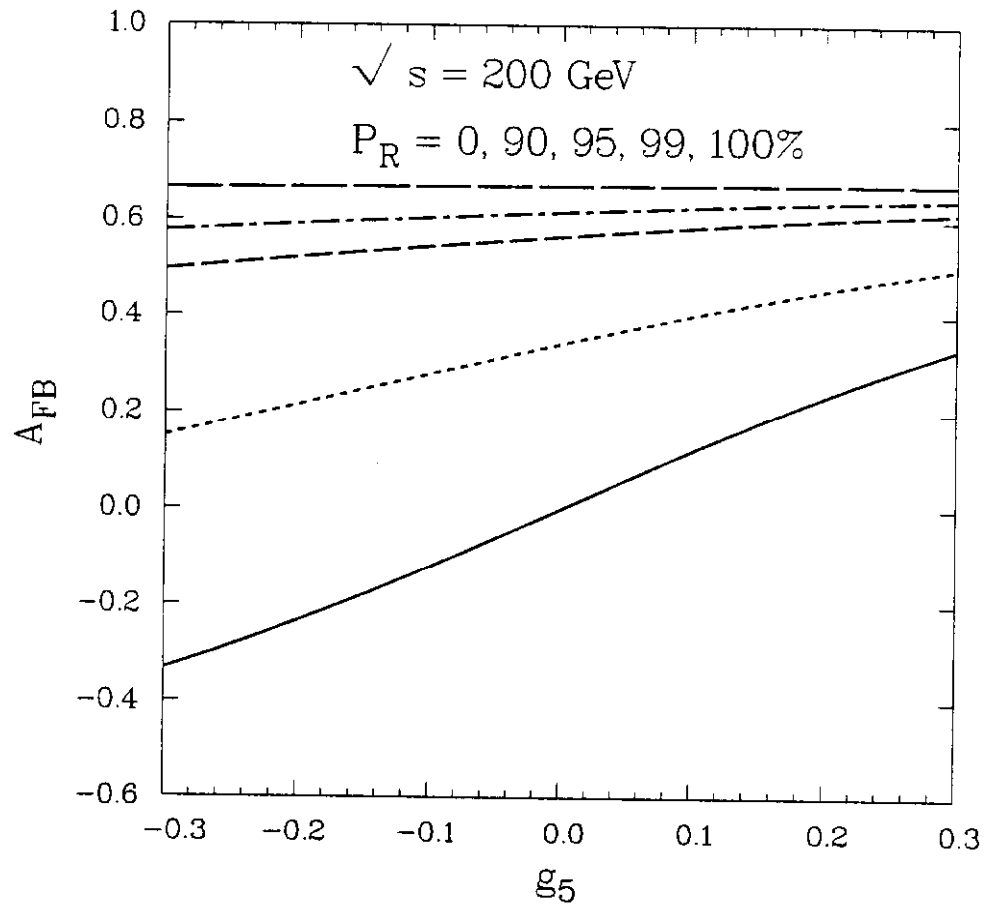


Figure 5b

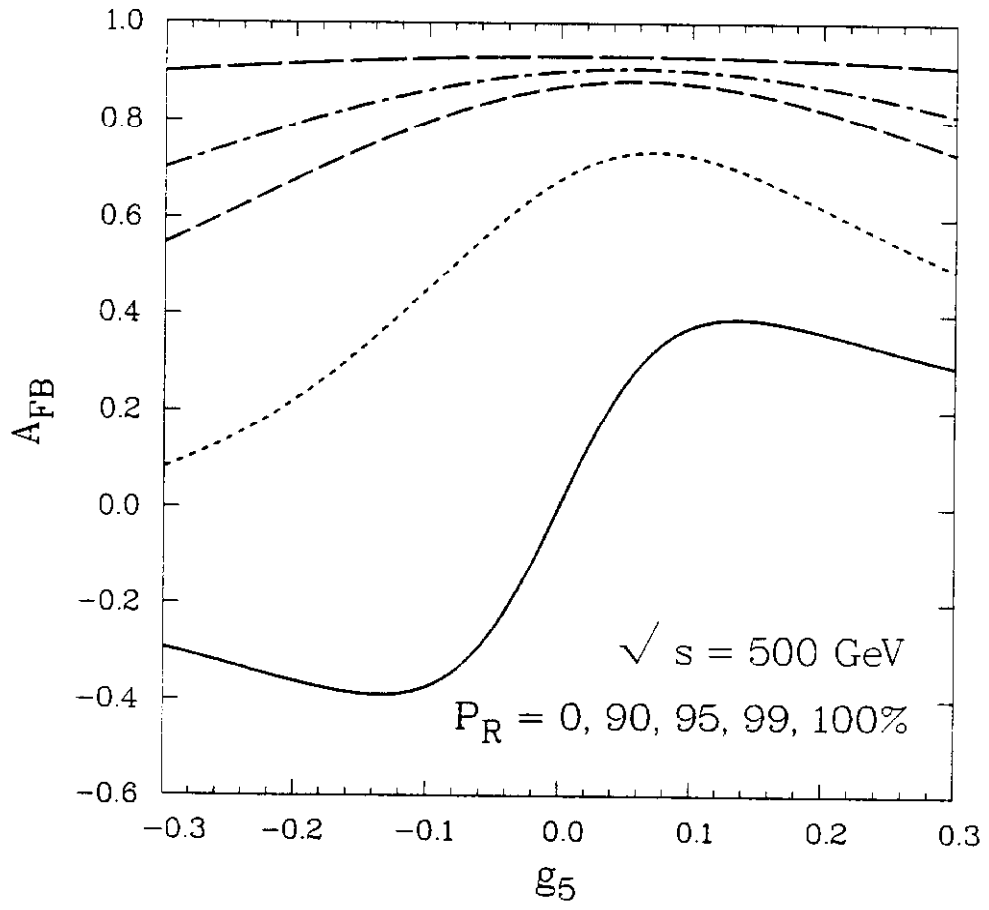


Figure 5c

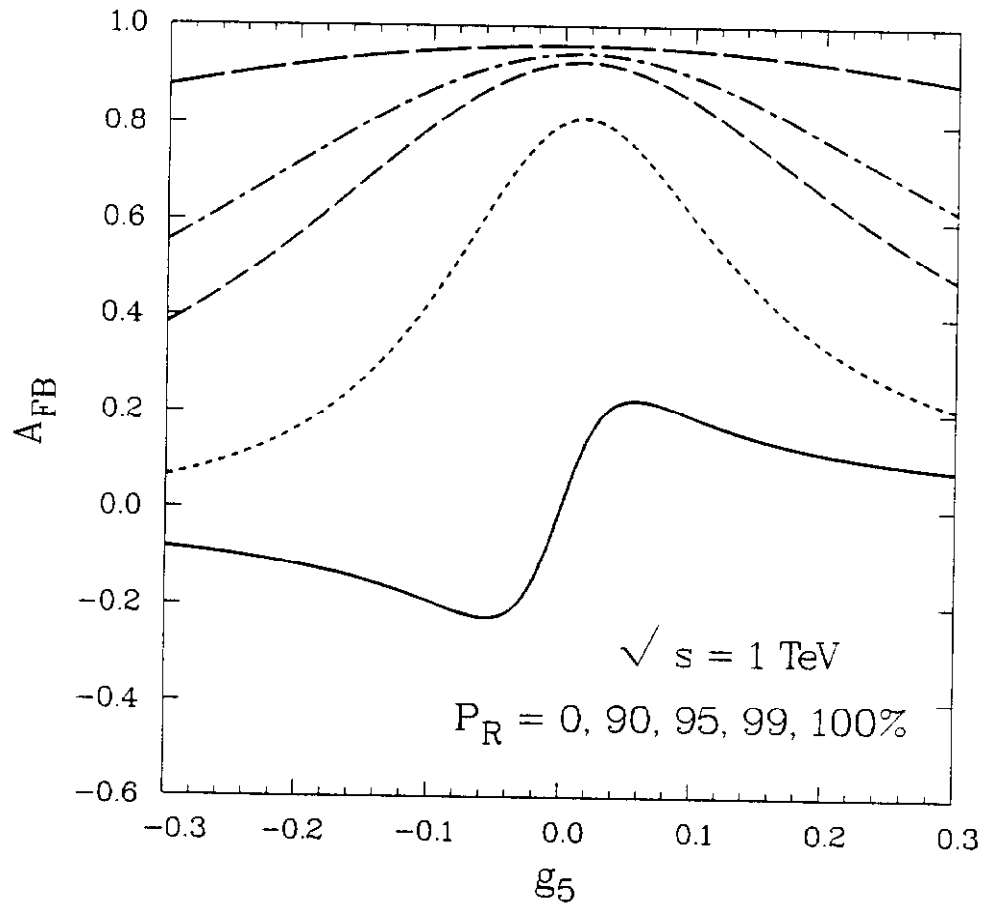


Figure 7

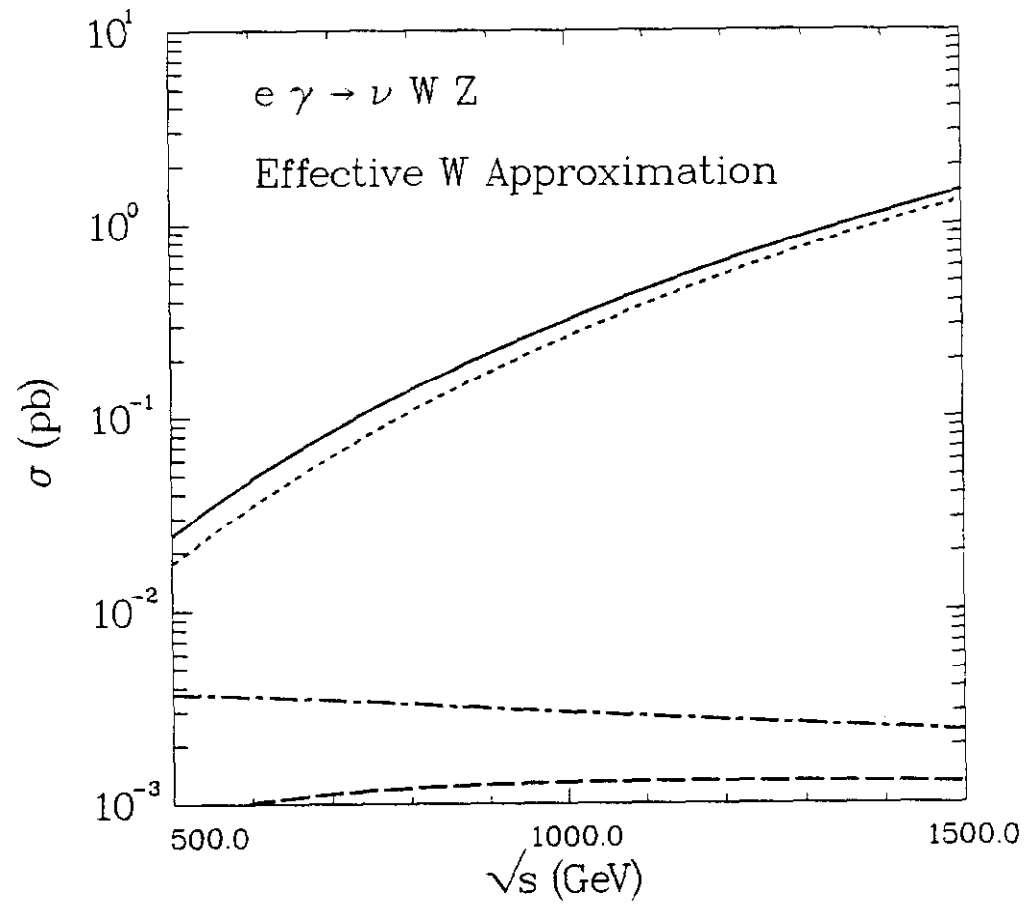


Figure 9

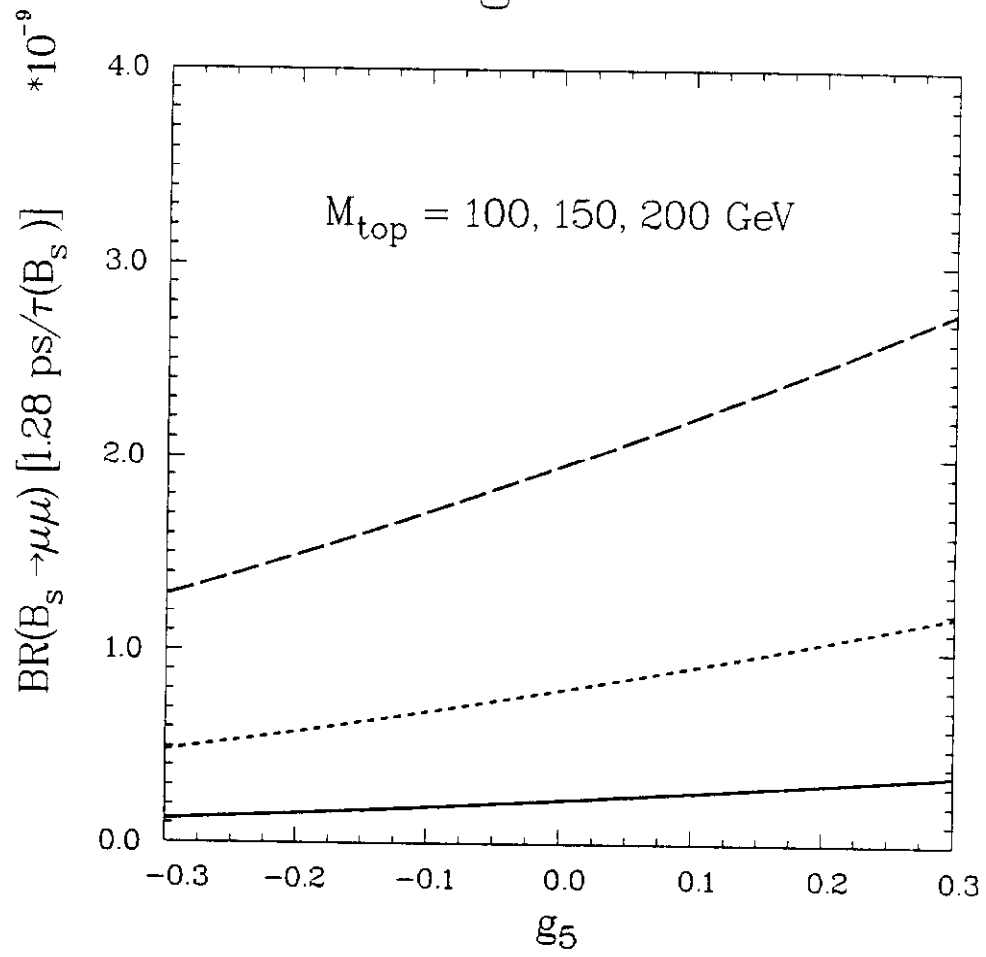


Figure 10

